Chemical Vapor Deposition of MoS_2 and TiS_2 Films From the Metal−Organic Precursors Mo(S-*t*-Bu)$_4$ and Ti(S-*t*-Bu)$_4$

Jinwoo Cheon, John E. Gozum, and Gregory S. Girolami*

School of Chemical Sciences and Materials Research Laboratory, University of Illinois at Urbana−Champaign, 601 South Goodwin Avenue, Urbana, Illinois 61801

Received March 7, 1997. Revised Manuscript Received May 20, 1997[⊗]

The deposition of MoS_2 and TiS_2 thin films from the metal-organic precursors Mo(S-*t*-Bu)$_4$ and Ti(S-*t*-Bu)$_4$ has been investigated. Stoichiometric films with low levels of oxygen and carbon contaminants can be grown at temperatures between 110 and 350 °C and low pressure. The films are amorphous when grown at these low temperatures and have granular morphologies in which the grains are 30−90 nm in diameter, the larger grain sizes being observed at higher deposition temperatures. For the MoS_2 deposits, the electrical conductivity was $\sim$1 Ω^{-1}cm^{-1}. For both precursors, the organic byproducts generated during deposition consist principally of isobutylene and *tert*-butylthiol; smaller amounts of hydrogen sulfide, isobutane, di-*tert*-butyl sulfide, and di-*tert*-butyl disulfide are also generated. A β-hydrogen abstraction/proton-transfer mechanism accounts for the distributions of the organic byproducts seen during the deposition of MoS_2 and TiS_2 films. Our results differ in some respects from those of a previous study of the deposition of thin films from the titanium thiolate precursor.

Introduction

The technological applications of transition-metal chalcogenides are many and are the principal driving forces behind much of the interest in these solid-state compounds. Layered transition-metal dichalcogenide compounds are especially versatile;[1,2] the weak van der Waals bonding between the layers makes these compounds useful for such diverse applications as high-temperature lubricants,[3] hydrogenation catalysts,[4] and high-energy density batteries.[5] In addition, these materials exhibit a wide range of electronic properties; they can be semiconductors (TiS_2, MoS_2), semimetals ($TiSe_2$, WTe_2), or superconductors (TaS_2).[6]

Molybdenum disulfide is an excellent solid lubricant for high-precision space-borne applications such as satellite bearings, gears, and gimbals operating under extreme temperature ranges.[7,8] Its optical and electronic properties also make it a candidate for efficient solar energy cells,[9,10] and it has also been investigated as a cathode in high-density lithium batteries.[11,12] MoS_2 thin films have been prepared by a variety of techniques such as radio frequency sputtering,[13] pulsed laser evaporation,[14,15] chemical vapor transport,[16] and metal−organic chemical vapor deposition (MOCVD).[17] In the latter case, $Mo(CO)_6$ and H_2S were used as the chemical precursors.

Titanium disulfide is of interest because it is one of the most effective cathode materials in high-energy, rechargeable batteries[18−22] and because it is a solid lubricant that provides electrical contact.[23] The bulk form of TiS_2 has been synthesized from the elements at 1000−1100 °C in an evacuated quartz bomb,[24,25] and by chemical vapor transport using iodine as a transport agent over a temperature gradient of 800−720 °C.[26−30] An amorphous form of TiS_2 has also been prepared by

⊗ Abstract published in *Advance ACS Abstracts,* July 1, 1997.

(1) Coehoorn, R.; Hass, C.; Dijikstra, J.; Flipse, C. J. F.; deGroot, R. A.; Wold, A. *Phys. Rev. B* **1987**, *35*, 6195−6206.
(2) Whittingham, M. S. *Prog. Solid State Chem.* **1978**, *12*, 41−99.
(3) Fleischauer, P. D.; Lince, J. R.; Bertrand, P. A.; Bauer, R. *Langmuir* **1989**, *5*, 1009−1015.
(4) Pecoraro, T. A.; Chianelli, R. R. *J. Catal.* **1981**, *67*, 430−445.
(5) *Lithium Batteries*; Gabano, J. P., Ed.; Academic Press: London, 1983.
(6) Friend, R. H.; Yoffe. A. D. *Adv. Phys.* **1987**, *36*, 1−94.
(7) Singer, I. L. *Mater. Res. Soc. Symp. Proc.* **1989**, *140*, 215−226.
(8) Sliney, H. E. *Tribol. Int.* **1982**, *15*, 303−313.
(9) Pramanik, P.; Bhattacharya, S. *Mater. Res. Bull.* **1990**, *25*, 15−23.
(10) Simon, R. A.; Ricco, A. J.; Harrison, J.; Wrighton, M. S. *J. Phys. Chem.* **1983**, *87*, 4446−4453.
(11) Shin, H.; Doerr, J.; Deshpandey, C. V.; Dunn, B.; Bunshah, R. F. *Surf. Coat. Technol.* **1989**, *39/40*, 683−690.
(12) Auborn, J. J.; Barberio, Y. L.; Hanson, K. J.; Schleich, D. M.; Martin, M. J. *J. Electrochem. Soc.* **1987**, *134*, 580−586.
(13) Bichsel, R.; Levy, F. *J. Phys. D: Appl. Phys.* **1986**, *19*, 1809−1819.
(14) Donley, M. S.; McDevitt, N. T.; Hass, T. W.; Murray, P. T.; Grant, J. T. *Thin Solid Films* **1989**, *168,* 335−344.
(15) Donley, M. S.; Murray, P. T.; Barber, S. A.; Hass, T. W. *Surf. Coat. Technol.* **1988**, *36*, 329−340.
(16) Chatzitheodorou, G.; Fiechter, S.; Kunst, M.; Luck, J.; Tributsch, H. *Mater. Res. Bull.* **1988**, *23*, 1261−1271.
(17) Hoffman, W. K. *J. Mater. Sci.* **1988**, *23*, 3981−3986.
(18) Whittingham, M. S. *Science* **1976**, *192*, 1126−1127.
(19) Murphy, D. W.; Christian, P. A. *Science* **1979**, *205*, 651−656.
(20) Meunier, G.; Dormoy, R.; Levasseur, A. *Mater. Sci. Eng.* **1989**, *B3*, 19−23.
(21) Nazri, G.; MacArther, D. M.; Ogara, J. F. *Chem. Mater.* **1989**, *1*, 370−374.
(22) Scrosati, B. *Electrochim. Acta*. **1981**, *26*, 1559−1567.
(23) Haltner, A. J.; Oliver, C. S. *J. Chem. Eng. Data* **1961**, *6*, 128−130.
(24) Hahn, H.; Harder, B. *Z. Anorg. Allg. Chem.* **1956**, *288*, 241−256.
(25) Hahn, H.; Ness, P. *Z. Anorg. Allg. Chem.* **1959**, *302*, 17−36.
(26) Conroy, L. E. *Inorg. Synth.* **1970**, *12*, 158−165.
(27) Rimmington, H. P. B.; Balchin, A. A.; Tanner, B. K. *J. Cryst. Growth* **1972**, *15*, 51−56.
(28) Rimmington, H. P. B.; Balchin, A. A. *J. Cryst. Growth* **1974**, *21*, 171−181.
(29) Saeki, M. *J. Cryst. Growth*, **1976**, *36*, 77−82.
(30) Dutrizac, J. E. *J. Less-Common Met.* **1977**, *51*, 283−303.

S0897-4756(97)00138-5 CCC: $14.00 © 1997 American Chemical Society

a metathesis reaction of $TiCl_4$ with Li_2S.[31] Thin films of TiS_2 have been prepared in several ways, including radio frequency sputtering from $TiCl_4$ and H_2S,[32] activated reactive evaporation or direct sulfurization from Ti and H_2S,[33] and plasma-assisted or thermal CVD from titanium chloride and hydrogen sulfide at temperatures above 400 °C.[34−38] Recently, CVD of TiS_2 was reported by using $TiCl_4$ and *tert*-butylthiol in a hot-walled reactor at temperatures as low as 200 °C.[39,40] In addition, thin films of TiS_2 have been prepared by treating $TiCl_4$ and various sulfur sources such as bis(trimethylsilyl) sulfide, di-*tert*-butyl sulfide, or di-*tert*-butyl disulfide at temperatures between 200 and 550 °C.[41]

There is a report that thin films of titanium monosulfide, TiS, can be prepared by a MOCVD route from the single source precursor Ti(S-*t*-Bu)$_4$ at temperatures between 130 and 200 °C.[42] The resulting purplish film was identified as amorphous TiS on the basis of energy-dispersive X-ray spectroscopy (EDX) and X-ray diffraction. The reduction of the titanium center from the +4 to the +2 oxidation state was accompanied by the formation of di-*tert*-butyl sulfide, di-*tert*-butyl disulfide, and a small amount of butane. The identification of the product as TiS is somewhat surprising; TiS_2 would seem to be the more reasonable product at temperatures below 200 °C since titanium is not easily reduced to the +2 oxidation state. Since EDX is unable to detect elements of low atomic number,[43] the amounts of carbon and oxygen present in the films were not measured. In any event, the composition of the films obtained from Ti(S-*t*-Bu)$_4$ is open to some doubt.

We now describe the chemical vapor deposition of molybdenum disulfide and titanium disulfide films from the metal−organic precursors Mo(S-*t*-Bu)$_4$ and Ti(S-*t*-Bu)$_4$. Mechanistic aspects of the decomposition pathways are also described.

Results and Discussion

Deposition of MoS_2 Films. Although there are few volatile compounds that contain both molybdenum and sulfur, one compound in particular is potentially well-suited as a single-source precursor to molybdenum sulfide phases: the *tert*-butyl thiolate Mo(S-*t*-Bu)$_4$ first

(31) Chianelli, R. R.; Dines, M. B. *Inorg. Chem.* **1978**, *17*, 2758−2762.
(32) Meunieier, G.; Doromoy, R.; Levasseur, A. *Mater. Sci. Eng.* **1989**, *B3*, 19−23.
(33) Zehnder, D.; Deshpandey, C.; Dunn, B.; Bunshah, R. F. *Solid State Ionics* **1986**, *18/19*, 813−817.
(34) Kikkawa, S.; Miyazaki, M.; Koizumi, M. *J. Mater. Res.* **1990**, *5*, 2894−2901.
(35) Kikkawa, S.; Shimanouchi-Futagami, R.; Koizumi, M. *Appl. Phys.* **1989**, *A49*, 105−109.
(36) Kanehori, K.; Ito, Y.; Kirino, F.; Miyauchi, K.; Kudo, T. *Solid State Ionics* **1986**, *18/19*, 818−822.
(37) Motojima, S.; Itoh, K.; Takahashi, Y.; Sugiyama, K. *Bull. Chem. Soc. Jpn.* **1978**, *51*, 3240−3244.
(38) Kanehori, K.; Kirino, F.; Ito, Y.; Miyauchi, K.; Kudo, T. *J. Electrochem. Soc.* **1989**, *136*, 1265−1270.
(39) Winter, C. H.; Lewkebandara, T. S.; Proscia, J. W. *Chem. Mater.* **1992**, *4*, 1144−1146.
(40) Lewkebandara, T. S.; Winter, C. H. *Adv. Mater.* **1994**, *6*, 237−239.
(41) Chang, H. S. W.; Schleich, D. M. *J. Solid State Chem.* **1992**, *100*, 62−70.
(42) Bochmann, M.; Hawkins, I.; Wilson, L. M. *J. Chem. Soc., Chem. Commun.* **1988**, 344−345.
(43) Goldstein, J. I.; Newburg, D. E.; Echlin, P.; Joy, D. C.; Fiori, C.; Lifshin, E. *Scanning Electron Microscopy and X-ray Microanalysis*; Plenum: New York, 1981; Chapters 5, 6.

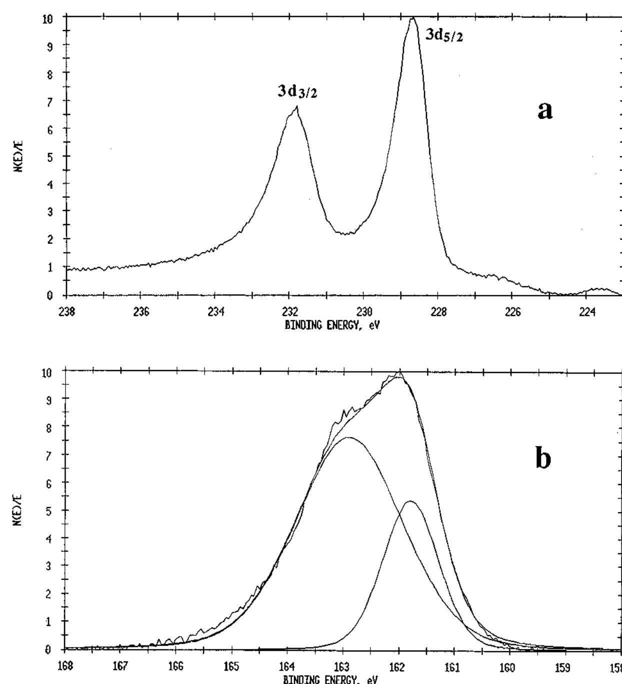

Figure 1. X-ray photoelectron spectrum of MoS_2 film grown from Mo(S-*t*-Bu)$_4$ at 200 °C on quartz: (a) in the Mo 3d region; the small shoulder at 226.41 eV is the sulfur 2s peak (b) in the S 2p region.

prepared by Otsuka.[44] This air-sensitive compound is easily prepared and sublimes readily in vacuum at 45 °C. The deposition of films from Mo(S-*t*-Bu)$_4$ was carried out at substrate temperatures between 110 and 350 °C and at a pressure of 10^{-4} Torr, by using a Pyrex high-vacuum apparatus containing a resistively heated hot stage. Passage of Mo(S-*t*-Bu)$_4$ over substrates such as quartz, silicon wafers, and stainless steel under these conditions resulted in the deposition of reflective dark brown films; below 110 °C, no deposition takes place. The film thickness depends on the deposition time and total flux of precursor, but typically a 1.0 μm thick film was grown in several hours from 0.3 g of the precursor at 200 °C.

X-ray powder diffraction analysis of the films showed broad scattering in the 10−30° (2θ) region, which is characteristic of an amorphous deposit. X-ray photoelectron spectroscopy (XPS) analyses of a sample prepared at 200 °C showed that significant amounts of carbon and oxygen were present at the surface of the film; however, the intensities of O and C peaks are reduced considerably upon sputtering into the interior of the film.[45,46] An XPS spectrum recorded after sputtering through this overlayer showed a Mo $3d_{5/2}$ binding energy of 228.62 eV and a Mo $3d_{3/2}$ binding energy of 231.82 eV (Figure 1a); these are nearly identical with with the binding energies of 228.72 and 231.88 eV reported for polycrystalline MoS_2.[45,47,48] Peaks due to molybdenum oxides (MoO_2, MoO_3) were absent.[45,47] The

(44) Otsuka, S.; Kamata, M.; Hirotsu, K.; Higuchi, T. *J. Am. Cem. Soc.* **1981**, *103*, 3011−3023.
(45) Wagner, C. D.; Riggs, W. M.; Davis, L. E.; Moulder, J. F.; Muildenberg, G. E. *Handbook of X-ray Photoelectron Spectroscopy*; Perkin-Elmer: Eden Prairie, MN, 1978.
(46) Briggs, D.; Seah, M. P. *Practical Surface Analysis*; Wiley: Chichester, 1983.
(47) Stewart, T. B.; Fleischauer, P. D. *Inorg. Chem.* **1982**, *21*, 2426−2431.
(48) Grim, S. O.; Matienzo, L. J. *Inorg. Chem.* **1975**, *14*, 1014−1018.

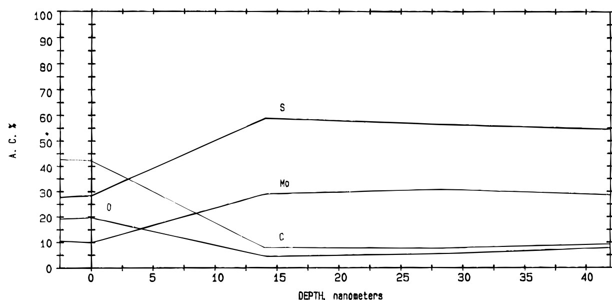

Figure 2. Depth profile (from Auger electron spectra) of a MoS_2 film grown from $Mo(S\text{-}t\text{-}Bu)_4$ on quartz at 200 °C.

sulfur 2p peak, which appeared as a broad envelope consisting of two peaks at 162.9 and 161.79 eV (Figure 1b), is also consistent with the presence of MoS_2 and clearly indicates that other sulfur species such as MoS_3 or SO_2 are absent.[45,47,49] The C 1s peak at 284.6 eV shows that the carbon-containing impurities in the films are not carbidic (i.e., MoC_x) but graphitic.[45]

The stoichiometries of the films deposited at 200 °C were determined by means of Auger electron spectroscopy (AES). The depth profile (Figure 2) shows that the S/Mo ratio is approximately 2, that about 6 atom % carbon is present and that oxygen levels are below the detection limit (<3%). In agreement with the XPS analyses, the highly asymmetric carbon peak at ca. 273 eV is indicative of the presence of graphitic carbon.[50−52]

It is clear that some hydrocarbon fragments must have been trapped in the film during the deposition process. Interestingly, analysis of a series of films deposited between 110 and 350 °C shows that the amount of carbon incorporated into the films does not change appreciably with temperature. We have also carried out depositions in the presence of H_2, since dihydrogen has been shown to reduce the amount of carbon present in other MOCVD-deposited films.[53,54] Films grown at hot-zone temperatures of 110 and 200 °C and at a H_2 flow rate of 25 sccm exhibited Mo and S XPS binding energies corresponding to MoS_2, but no significant decrease in the amount of carbon present was observed.

The electrical conductivities of the amorphous MoS_2 films deposited at 200 °C were very near 1.0 Ω^{-1} cm^{-1} at room temperature, a value very similar to those reported for polycrystalline MoS_2 thin films (ca. 10^{-3}–10^{1} Ω^{-1} cm^{-1}).[12,16] The morphologies of the MoS_2 films were studied by scanning electron microscopy (SEM). All of the films consisted of closely packed granules (Figure 3), with higher temperatures giving larger grain sizes: 90 nm in diameter at 200 °C compared to 30 nm at 110 °C. Similar temperature-dependent grain sizes were seen for the deposition of MoS_2 polycrystalline films by RF sputtering.[12] This behavior probably means that the rate of deposition increases more quickly with temperature than does the rate of nucleation.

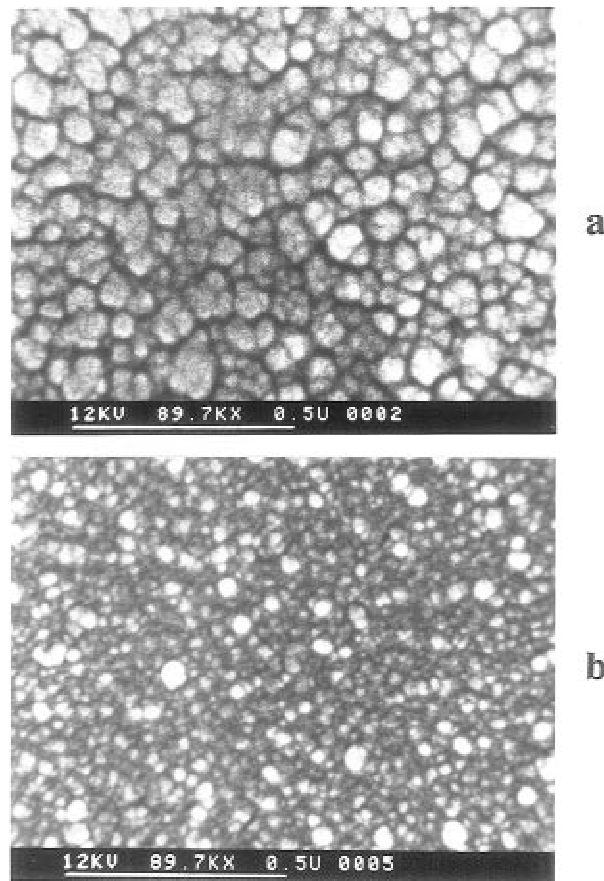

Figure 3. Scanning electron micrograph of a MoS_2 film grown from $Mo(S\text{-}t\text{-}Bu)_4$ on quartz (a) at 200 °C and (b) at 110 °C.

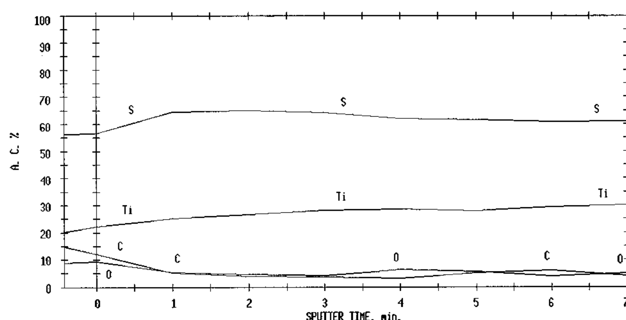

Figure 4. Depth profile (from Auger electron spectra) of a TiS_2 film grown from $Ti(S\text{-}t\text{-}Bu)_4$ on quartz at 270 °C.

Deposition of TiS_2 Films. We have reinvestigated the deposition of titanium sulfide films from the titanium complex $Ti(S\text{-}t\text{-}Bu)_4$ first reported by Bochmann et al.[42] Passage of $Ti(S\text{-}t\text{-}Bu)_4$ over quartz, silicon, and stainless steel substrates at temperatures of 150 and 270 °C and at a pressure of 10^{-4} Torr resulted in the deposition of gray-blue films. The film composition and morphology do not change appreciably as a function of deposition temperature within the range indicated. X-ray power diffraction (XRD) revealed that the films were amorphous. The AES depth profile results (Figure 4) indicated that the film stoichiometries were very close to TiS_2 and that small amounts of oxygen (ca. 4%) and carbon (<3%) were present. Examination of the films by XPS showed that that the Ti $2p_{3/2}$ binding energy was 456.5 eV and the S 2p binding energy was 161.3 eV; these values closely match those of 456.4 and 160.9 eV, respectively, reported for polycrystalline TiS_2.[45,55,56] We did *not* observe a Ti $2p_{3/2}$ peak at 454.4 eV that

(49) Stevens, G. C.; Edmond, T. *J. Catal.* **1975**, *37*, 544−547.
(50) Grant, J. T; Hass, T. W. *Surf. Sci.* **1971**, *24*, 332−344.
(51) Hass, T. W.; Grant, J. T.; Dooley, III, G. J. *J. Appl. Phys.* **1972**, *43*, 1853−1860.
(52) Ducros, R.; Piquard, G.; Weber, B.; Cassuto, A. *Surf. Sci.* **1976**, *54*, 513−518.
(53) Koplitz, L. V.; Shuh, D. K.; Chen, Y.; Willams, R. S.; Zink, J. I. *Appl. Phys. Lett.* **1988**, *53*, 1705−1707.
(54) Xue, Z.; Strouse, J.; Shuh, D. K.; Knobler, C. B.; Kaesz, H. D.; Hicks, R. F.; Williams, R. S. *J. Am. Chem. Soc.* **1989**, *111*, 879−884.

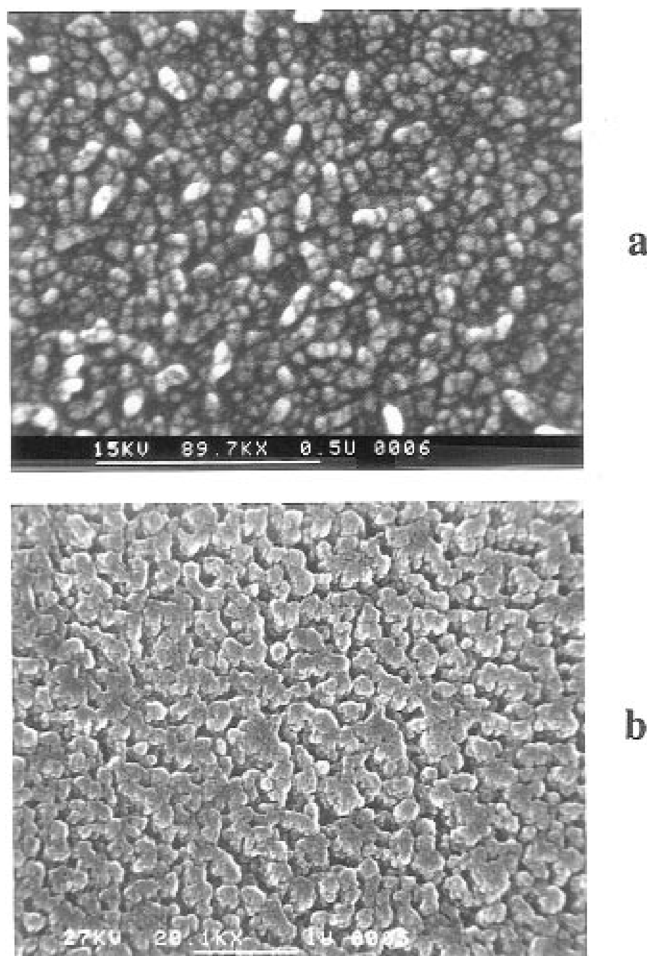

Figure 5. Scanning electron micrograph of a TiS_2 film grown from $Ti(S\text{-}t\text{-}Bu)_4$ on quartz (a) at 270 °C and (b) at 150 °C.

would indicate the presence of TiS.[45,56] Scanning electron microscopy (SEM) showed that the films consisted of homogeneous, very fine granules with diameters of ca. 40 nm (Figure 5).

Analysis of the Organic Byproducts Formed during Deposition. To gain some insight into the mechanisms by which metal disulfide films are deposited from these single-source thiolate precursors, we have analyzed the byproducts formed during deposition. In situ quadrupole mass spectroscopic analyses of the gases exiting the hot zone during a CVD run indicated that, for both $Mo(S\text{-}t\text{-}Bu)_4$ and $Ti(S\text{-}t\text{-}Bu)_4$, isobutylene and *tert*-butylthiol were the major byproducts and that H_2S was a minor product.

To establish the amounts of the byproduts formed, depositions were conducted in a closed static vacuum system where the gaseous byproducts could be collected quantitatively and analyzed. The precursors were sublimed under a static vacuum through a deposition zone heated to 200 °C (Mo) or 250 °C (Ti), and the gaseous byproducts were collected in a liquid N_2 cooled NMR tube as they were formed. After each deposition run was complete, the NMR tube was charged with a known amount of a benzene/benzene-d_6 mixture and the tube contents were analyzed by NMR spectroscopy. Although the conditions (particularly pressure and residence times) in the static vacuum apparatus differ somewhat from those in a flow-through CVD reactor, in fact the same organic byproducts are generated (and thus similar chemical reactions are taking place), as the following sections will show.

For the MoS_2 depositions, quantitative NMR analyses of the volatile byproducts generated in the static vacuum apparatus showed that 2.06 equiv of isobutylene, 1.57 equiv of *tert*-butylthiol, and 0.47 equiv of H_2S were generated per equivalent of $Mo(S\text{-}t\text{-}Bu)_4$ consumed. Trace amounts of di-*tert*-butyl sulfide (0.01 equiv), di-*tert*-butyl disulfide (0.01 equiv), and isobutane (0.05 equiv) were also detected. Subsequent GC/MS analysis of the tube contents confirmed the identities of all of these byproducts. These byproducts account for over 90% of the carbon and hydrogen originally present in the precursor. The deposits grown under static vacuum have stoichiometry $MoS_{1.89}$, with some carbon and oxygen contaminations, as revealed by elemental analysis.

For the TiS_2 depositions, the NMR analyses showed that 1.78 equiv of isobutylene, 1.42 equiv of *tert*-butylthiol, and 0.14 equiv of hydrogen sulfide were generated per equivalent of $Ti(S\text{-}t\text{-}Bu)_4$ consumed; minor amounts of di-*tert*-butyl sulfide (0.09 equiv), di-*tert*-butyl disulfide (0.08 equiv), and isobutane (0.04 equiv) were also formed. These products account for over 80% of the carbon and hydrogen originally present in the precursor. The deposits grown under static vacuum have the stoichiometry $TiS_{1.9}$, with some carbon and oxygen contaminations, as revealed by elemental analysis. It is significant to point out that our product distribution differs from that previously described for the deposition of "TiS" from $Ti(S\text{-}t\text{-}Bu)_4$.[42]

The distributions of the organic byproducts generated during the depositions of MoS_2 and TiS_2 are very similar: in both cases, H_2S is a significant product and the ratio of isobutylene to *tert*-butylthiol is ~1.3:1.[57] Given the similarities of the product distributions, it is reasonable to conclude that similar mechanisms are responsible for the deposition of MoS_2 and TiS_2 from their respective *tert*-butylthiolate precursors. At least two different mechanisms could account for the observed product distributions, and these will be considered in turn.

***β*-Hydrogen Elimination/Proton-Transfer Mechanism.** The formation of isobutylene, *tert*-butyl thiol, and hydrogen sulfide as major byproducts in the deposition of MS_2 from $M(S\text{-}t\text{-}Bu)_4$ can be explained most simply by the following three surface reactions:

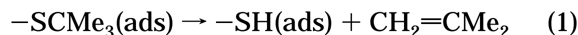

$$-SCMe_3(ads) \rightarrow -SH(ads) + CH_2{=}CMe_2 \quad (1)$$

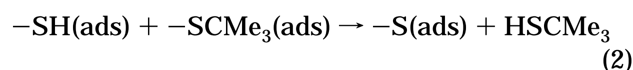

$$-SH(ads) + -SCMe_3(ads) \rightarrow -S(ads) + HSCMe_3 \quad (2)$$

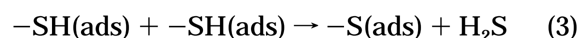

$$-SH(ads) + -SH(ads) \rightarrow -S(ads) + H_2S \quad (3)$$

In the first step, a *tert*-butyl thiolate ligand undergoes β-hydrogen elimination (possibly via a concerted intramolecular pathway),[58] resulting in C−S bond cleavage, elimination of isobutylene, and formation of an surface

(55) Fujinori, A.; Suga, S.; Negishi, H.; Inoue, M. *Phys. Rev. B* **1988**, *38*, 3676−3689.
(56) Itti, R.; Wada, T.; Matsuura, K.; Itoh, T.; Ikeda, K.; Yamauchi, H.; Koshizuka, N.; Tanaka, S. P. *Phys. Rev. B* **1991**, *44*, 2306−2312.

(57) Slightly larger amounts of minor products were detected from the deposition of TiS_2.

thiol (SH) species (eq 1). Subsequent transfer of the thiol hydrogen atom to an adjacent *tert*-butylthiolate ligand results in the formation of *tert*-butylthiol and a surface sulfide atom (eq 2). Alternatively (and competitively), transfer of the thiol hydrogen atom to a neighboring thiol group would generate hydrogen sulfide and a surface sulfide atom (eq 3). Very similar mechanisms have been proposed for reactions of some thiolate[58] and *tert*-butoxide complexes (*tert*-butoxide being the oxygen analogue of *tert*-butylthiolate).[59,60]

Equations 1–3 are attractive because they easily explain both the presence of H_2S among the gaseous byproducts[61] and the 1.3:1 ratio of isobutylene to *tert*-butylthiol. If only eqs 1 and 2 were operative, no H_2S would be formed and the isobutylene:*tert*-butylthiol ratio would be 1:1. Instead, the effect of eq 3 is to introduce a branch in the deposition pathway; the relative amounts of isobutylene, *tert*-butylthiol, and hydrogen sulfide suggest that, under our reaction conditions, the reaction described by eq 2 is 3–10 times faster than the reaction described by eq 3.

There are some relevant solution and surface studies of the cleavage of C–S bonds in transition-metal thiolate complexes.[62–67] Thermolysis of zirconium and niobium *tert*-butylthiolate complexes proceeds to give *tert*-butylthiol, isobutylene, and isobutane as organic byproducts.[62,63] The isobutylene was proposed to be generated via a two-step β-hydrogen elimination process involving heterolytic C–S bond cleavage followed by proton transfer from the *tert*-butyl carbonium ion to the metal-sulfide anion. In contrast, isobutane was proposed to be generated from homolytic C–S bond cleavage and subsequent hydrogen atom transfer from the *tert*-butyl radical. In addition, ultrahigh vacuum studies show that upon heating to 400 K, *tert*-butylthiolate groups bound to Mo(110) surfaces undergo β-hydrogen elimination to form isobutylene, C_α–S bond hydrogenolysis to form isobutane, and nonselective decomposition to form atomic carbon, atomic sulfur, and gaseous dihydrogen.[68] Similar C–S bond-cleavage processes are undoubtedly important in hydrodesulfurization catalysis.[69,70] These studies show (1) that the organic byproducts we observed can be formed directly from surface-bound thiolate groups, and (2) that alternative mechanisms for the deposition of MS_2 phases from the $M(S\text{-}t\text{-}Bu)_4$ precursors, such as primary formation of di-*tert*-butyl sulfide or di-*tert*-butyl disulfide and subsequent thermolysis of these species to the observed product distribution, can be ruled out.

Homolytic C–S bond[62] and Ti–S bond cleavage processes that generate *tert*-butyl and *tert*-butylthioyl radicals are known to terminate in the formation of isobutane, di-*tert*-butyl sulfide, and di-*tert*-butyl disulfide. The near absence of these species among the CVD byproducts strongly suggests that radical intermediates play a negligible role.

Taken together, these solution and surface studies support the contention that eqs 1–3 best describe the pathway by which metal disulfide films are deposited from $M(S\text{-}t\text{-}Bu)_4$ precursors.

Thiol Dehydrosulfurization Mechanism. Another mechanism that could account for the observed product distributions can be represented by the following three equations:

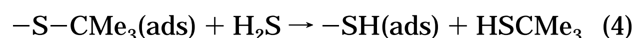

$$-S-CMe_3(ads) + H_2S \rightarrow -SH(ads) + HSCMe_3 \quad (4)$$

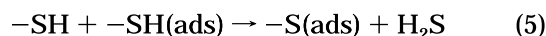

$$-SH + -SH(ads) \rightarrow -S(ads) + H_2S \quad (5)$$

$$HSCMe_3 \rightarrow CH_2{=}CMe_2 + H_2S \quad (6)$$

This mechanism differs from the β-hydrogen elimination/proton-transfer pathway in that isobutylene is formed as a secondary product via the dehydrosufurization of *tert*-butylthiol (eq 6). In addition, hydrogen sulfide plays a direct role in the formation of *tert*-butylthiol from surface-bound *tert*-butylthiolate groups (eq 4). A similar mechanism has been proposed for the decomposition of the *tert*-butoxide complex $Zr(O\text{-}t\text{-}Bu)_4$ in a closed constant-pressure system.[71–73] The dehydrosulfurization of organic thiols including *tert*-butylthiol is known to be catalyzed by both metal and sulfur-treated metal surfaces.[68,74]

To test whether this mechanism is occurring, we exposed *tert*-butylthiol to freshly deposited MoS_2 and TiS_2 films at 250 °C. After 20 min, the gases were collected and analyzed by ^1H, ^{13}C NMR, and GC/MS methods. The results showed that only small amounts of isobutylene and H_2S had been formed per equivalent of *tert*-butylthiol: for MoS_2, about 0.09 equiv of isobutylene and 0.08 equiv of H_2S, and for TiS_2, 0.04 equiv of isobutylene.[75] This result indicates that the dehydrosulfurization of *tert*-butylthiol is negligible for the contact times typical during CVD runs; i.e., the gases pass out of the hot zone in seconds and do not remain there long enough to convert *tert*-butylthiol to isobutylene to any significant degree.

Concluding Remarks

We have been unable to obtain purple films of composition TiS by CVD from $Ti(S\text{-}t\text{-}Bu)_4$ as reported by Bochmann,[42] and instead of di-*tert*-butyl sulfide and di-*tert*-butyl disulfide (which were the major organic byproducts in the earlier study) we find that isobutylene

(58) MacInnes, A. N.; Power, M. B.; Hepp, A. F.; Barron, A. R. *J. Organomet. Chem.* **1993**, *449*, 95–104.

(59) Nandi, M.; Rhubright, D.; Sen, A. *Inorg. Chem.* **1990**, *29*, 3065–3066.

(60) Jeffries, P. M.; Dubois, L. H.; Girolami, G. S. *Chem. Mater.* **1992**, *4*, 1169–1175.

(61) Somewhat more H_2S is detected than expected from the isobutylene:*tert*-butylthiol ratio. The amount of H_2S that is generated during these deposition studies is difficult to measure accurately, however, due to the small intensity of its ^1H NMR peak.

(62) Coucouvanis, D.; Al-Ahmad, S.; Kim, C. G.; Koo, S.-M. *Inorg. Chem.* **1992**, *31*, 2996–2998.

(63) Coucouvanis, D.; Lester, R. K.; Kanatzidis, M. G.; Kessissoglou, D. P. *J. Am. Chem. Soc.* **1985**, *107*, 8279–8280.

(64) Tatsumi, K.; Sekiguchi, Y.; Nakamura, A. *J. Am. Chem. Soc.* **1986**, *108*, 1358–1359.

(65) Boorman, P. M.; Chivers, T.; Mahadev, K. N. *Inorg. Chim. Acta* **1976**, *19*, L35–37.

(66) Kräuter, G.; Favreau, P.; Rees, W. S. *Chem. Mater.* **1994**, *6*, 543–549.

(67) Kräuter, G.; Neumüller, B.; Goedken, V. L.; Rees, W. S. *Chem. Mater.* **1996**, *8*, 360–368.

(68) Wiegand, B. C.; Uvdal, P.; Friend, C. M. *J. Phys. Chem.* **1992**, *96*, 4527–4533.

(69) Amberg. D. H. *J. Less-Common Met.* **1974**, *36*, 339–352.

(70) Stiefel, E. I.; Halbert, T. R.; Coyle, C. L.; Wei, L.; Pan, W. H.; Ho, T. C.; Chianelli, R. R.; Daage, M. *Polyhedron* **1989**, *18*, 1625–1629.

(71) Bradley, D. C.; Faktor, M. M. *Trans. Faraday Soc.* **1959**, *55*, 2117–2123.

(72) Bradley, D. C. *Chem. Rev.* **1989**, *89*, 1317–1322.

(73) Holzschuh, H.; Suhr, H. *Appl. Phys. A* **1990**, *51*, 486-490.

(74) Wiegand, B. C.; Friend, C. M. *Chem. Rev.* **1992**, *92*, 491–504.

(75) H_2S was not detectable by ^1H NMR spectroscopy. Its presence was established by GC/MS.

and *tert*-butylthiol are the principal byproducts, with di-*tert*-butyl sulfide and disulfide being formed only in trace amounts. It is possible that some of these contradicting observations reflect the action of water and dioxygen either during or after deposition. Hydrolysis of the films, especially if the films are microporous, can lead to the loss of sulfur and the incorporation of oxygen. Such a process might not be readily noticed, particularly since the oxygen contents of the films were not determined in the previous study. Oxidation could also account for the large amounts of di-*tert*-butyl sulfide and disulfide noted in the previous study, since these compounds can rather easily be generated by the reaction of *tert*-butylthiol with dioxygen at elevated temperatures (particularly in the presence of metal catalysts; it is possible that the deposited films were acting as catalysts in the prevous study). Finally, the *n*-butane said to be formed was undoubtedly isobutane, since these species cannot be easily distinguished by mass spectrometry (but are readily identifiable by NMR spectroscopy).

The three-step β-hydrogen elimination/proton-transfer mechanism (eqs 1−3) explains reasonably well the distributions of the organic byproducts seen during the deposition of MoS_2 and TiS_2 films from their corresponding metal−organic precursors. Other transition metal *tert*-butylthiolate complexes should also react similarly, and such compounds may in general prove to be useful MOCVD precursors for the deposition of metal sulfide thin films at relatively low temperatures.

Experimental Section

General Methods. All manipulations were carried out using standard Schlenk and cannula techniques under argon or in vacuum. Pentane was distilled from sodium benzophenone ketyl under N_2 before use. $MoCl_5$ (Cerac) was used as received. Titanium tetrachloride (Aldrich) and *tert*-butylthiol (Aldrich) were distilled before use.

Elemental analyses were performed by the School of Chemical Sciences Microanalytical Laboratory at the University of Illinois. ^{1}H and ^{13}C NMR spectra were recorded on a Varian Unity 400 instrument at 400 and 100.5 MHz, respectively. ^{1}H and ^{13}C NMR chemical shifts are reported in δ units (positive chemical shifts to higher frequency) and are referenced with respect to the NMR solvent, benzene-d_6 at δ 7.15 and 128, respectively. A Hewlett-Packard 5890 gas chromatography with a 5970 series mass-selective detector was used to obtain the GC/MS data. The mass selective detector was calibrated by using the 31, 50, and 69 amu peaks of perfluorotributylamine. The column used was a 30 m RSL-160 (5 μm thick poly(dimethylsiloxane) film, 0.32 mm i.d., Alltech).

X-ray photoelectron spectroscopy (XPS) experiments were performed on a Perkin-Elmer PHI-5400 ESCA system with a 15 kV, 400 W Mg Kα radiation source (1253.6 eV) under an operating pressure of ca. 10^{-10} Torr. The electron spectrometer was calibrated by the Au $f_{7/2}$ peak at 83.8 eV, and spectra were taken with a pass energy of 89.45 eV for the survey analysis and 17.9 eV for the multiplex analysis with an energy resolution of 0.5 eV. Auger electron spectroscopy (AES) experiments were performed on a Perkin-Elmer PHI-660 AES system with a beam energy of 3 kV and a beam current density of ca. 5 μA cm^{-2} under an operating pressure of ca. 10^{-10} Torr. XPS and AES spectra were collected after the samples had been Ar sputtered to remove surface contaminations. X-ray powder diffraction (XRD) data were recorded on a Rigaku D-Max instrument using Cu Kα radiation with a power supply of 40 kV and 20 mA. Scanning electron micrographs (SEM) were obtained on an ISI DS-130 instrument. Electrical conductivities were measured by painting silver electrodes (GC Electronics silver print conductive paint) on the film surface and measuring the film resistance with a four-point method. Film thicknesses were determined on a Dektak 3030 stylus profilometer. Tetrakis(*tert*-butylthiolato)molybdenum(IV), Mo(S-*t*-Bu)$_4$, was prepared by the literature method.[44]

Tetrakis(*tert*-butylthiolato)titanium(IV), Ti(S-*t*-Bu)$_4$. This procedure is a more detailed version of the literature method.[42] To a solution of $Ti(NEt_2)_4$[76] (3.04 g, 18.5 mmol) in pentane (30 mL) at 25 °C was added *tert*-butylthiol (20.9 mL, 185 mmol). Immediately upon addition of thiol, the solution became dark red. The pentane and excess *tert*-butylthiol were removed under vacuum, and the dark red residue was extracted with pentane (2 × 30 mL). The extracts were combined, filtered, and concentrated to ca. 10 mL. Cooling the red solution to −20 °C gave red microcrystals of the product, which can be further purified by sublimation at 50 °C and 10^{-4} Torr. Yield: 2.8 g (35%). Anal. Calcd for $C_{16}H_{36}S_4Ti$: C, 47.5; H, 8.97; S, 31.7. Found: C, 46.7; H, 8.82; S, 27.3. ^{1}H NMR (C_6D_6, 25 °C) δ 1.75 (s, CMe$_3$). ^{13}C NMR (C_6D_6, 25 °C) δ 58.9 (s, *C*Me$_3$), 36.2 (s, C*Me*$_3$).

MOCVD Apparatus. The low-pressure (10^{-4} Torr) apparatus used to carry out the film depositions is a hot-wall 5 cm diameter horizontal tube design and has been described elsewhere.[77] The precursor was introduced into the Pyrex vacuum system via a break seal ampule after the system had been baked out at 200 °C and ca. 10^{-4} Torr for 24 h. The substrates were mounted on a resistively heated stage whose temperature was monitored with a thermocouple. A gas-flow controller allowed gases such as H_2 to be metered into the reactor during deposition. A quadrupole mass spectrometer, interfaced to the system just downstream of the hot zone, allowed in situ analysis of the gaseous products generated during deposition. The precursor reservoir and glass tubing to the deposition zone were maintained at 45 °C to provide a satisfactory transport rate and to prevent the precursors from condensing. Quartz slides (washed with dilute HCl, ethanol, acetone, and pentane and then air-dried), silicon wafers [Monsanto, n-doped, (100) orientation, 15 mil thickness], and stainless steel (type 316, 1.5 cm diameter disks cut from $^1/_{16}$ in. thick sheets; washed with dilute HCl, ethanol, acetone, and pentane and then air-dried) were used as substrates.

Chemical Vapor Deposition of MoS_2 Thin Films. The depositions of MoS_2 were conducted at the following hot zone temperatures: 110, 160, 200, and 350 °C. The MoS_2 films obtained were reflective and dark brown in appearance. Typically, the deposition time was several hours and films of up to about a micron in thickness were grown at 200 °C from 0.3 g of precursor. Very little of the precursor remained unsublimed at the end of the deposition runs.

For comparison, some depositions were conducted in the presence of a H_2 carrier. The dihydrogen flow rate was 25 cm^3/min (sccm), and the system pressure was ca. 10^{-2} Torr.

Chemical Vapor Deposition of TiS_2 Thin Films. The depositions of TiS_2 films were carried at substrate temperatures of 150, 250, and 270 °C. The depositions of TiS_2 were carried out as described above except that after the system had been baked out for 24 h, $TiCl_4$ (ca. 0.4 mL) was slowly introduced into the CVD chamber to remove surface-bound water. After ca. 20 min, the unreacted $TiCl_4$ was condensed into a liquid nitrogen trap, and the deposition run was started. The TiS_2 deposits were gray-blue in appearance. Typically, the deposition time was 2 h and films of up to about a micron in thickness were grown at 270 °C. Very little of the precursor remained unsublimed at the end of the deposition runs.

Static Vacuum CVD Studies and Analysis of Gaseous Byproducts. To collect and analyze quantitatively the gaseous products generated during film deposition, the precursors were thermolyzed under a static vacuum (10^{-3} Torr) at 200−250 °C in a closed-system CVD apparatus. This apparatus consisted of a solvent reservoir, a precursor reservoir, a deposition zone, and an NMR tube and is described more fully elsewhere.[60] The solvent reservoir was charged with a mixture

(76) Bradley, D. C.; Thomas, I. M. *J. Chem. Soc.* **1960**, *82*, 3857−3861.

(77) Gozum, J. E. Ph.D. Thesis, University of Illinois at Urbana−Champaign, 1991.

of degassed benzene and benzene-d_6 (1.440×10^{-2} mol of protons/g of solvent). During the thermolysis step, the solvent reservoir was isolated from the rest of the apparatus.

The precursor reservoir was charged with Mo(S-*t*-Bu)$_4$ (0.190 g, 0.42 mmol) and cooled to −78 °C. The apparatus was evacuated to 10^{-2} Torr and the hot zone was heated externally to 200 °C; after bake-out, the apparatus was isolated from the pump and kept under a static vacuum. The NMR tube was cooled to −196 °C, and the precursor reservoir was heated to 45 °C to sublime the Mo(S-*t*-Bu)$_4$ through the deposition zone. A dark brown film deposited on the walls of the deposition zone and the volatile byproducts were collected in the NMR tube. After the precursor had sublimed and the deposition was complete, the deposition zone was cooled to room temperature. The benzene/benzene-d_6 mixture (0.481 g) in the solvent reservoir was transferred into the liquid nitrogen cooled NMR tube. The NMR tube was flame sealed and the contents were analyzed by ^{1}H and ^{13}C NMR spectroscopy. Integration errors due to differences in spin−lattice relaxation times were minimized by using postacquisition delays greater than 5 times the longest T_1 and, for ^{13}C NMR spectra, NOE effects were suppressed by turning the decoupler off between acquisitions.

The ^{1}H and ^{13}C NMR spectra of the organic products from the static vacuum CVD experiment showed the presence of *tert*-butylthiol and isobutylene along with trace amounts of di-*tert*-butyl sulfide, di-*tert*-butyl disulfide, and isobutane. From the relative intensities of the $C_6\mathit{H}_6$, $Me_2C{=}C\mathit{H}_2$, and H_2S peaks in the ^{1}H NMR spectrum (17.43:4.29:1.00) and the known concentration of protons in the benzene/benzene-d_6 mixture, it was established that 8.60×10^{-4} mol of isobutylene and 1.98×10^{-4} mol of hydrogen sulfide had been generated. Since peaks due to *tert*-butylthiol, di-*tert*-butyl sulfide, di-*tert*-butyl disulfide, and isobutane overlap in the ^{1}H NMR spectrum, the amounts of these species present were determined from integration of their $^{13}C\{^1H\}$ NMR resonances. The relative intensities of the Me_3CSH, $\mathit{Me}_2C{=}CH_2$, $HC\mathit{Me}_3$, $S(C\mathit{Me}_3)_2$, and $S_2(C\mathit{Me}_3)_2$ peaks (59.0:51.3:2.0:1.1:1.0), combined with the calibrated peak integrals from the ^{1}H NMR data, established that 6.60×10^{-4} mol of *tert*-butylthiol, 5.5×10^{-6} mol of di-*tert*-butyl sulfide, 5.7×10^{-6} mol of di-*tert*-butyl disulfide, and 2.2×10^{-5} mol of isobutane had been generated. After NMR analysis of the byproducts, the sealed NMR tube was broken and the contents were analyzed by GC/MS. The identities of the byproducts detected by NMR spectroscopy were confirmed: the cracking patterns seen by mass spectrometry agreed with those in the literature.[78]

The static vacuum thermolysis of TiS_2 was carried out using the same procedureas above, except that the deposition zone was maintained at 250 °C. Amounts of reagents used: Ti(S-*t*-Bu)$_4$ (0.207 g, 0.51 mmol), benzene/benzene-d_6 (0.453 g). The ^{1}H and ^{13}C NMR spectra of the organic products from the static vacuum CVD experiment showed the presence of *tert*-butylthiol and isobutylene along with trace amounts of di-*tert*-butyl sulfide, di-*tert*-butyl disulfide, and isobutane. The relative intensities of the $C_6\mathit{H}_6$, $Me_2C{=}C\mathit{H}_2$, and H_2S peaks in the ^{1}H NMR spectrum (46.92: 13.08:1.00) and the Me_3CSH, Me_2CCH_2, $S(C\mathit{Me}_3)_2$, $S_2(C\mathit{Me}_3)_2$, and $HC\mathit{Me}_3$ peaks in the $^{13}C\{^1H\}$ NMR spectrum (34.20:28.50:4.45:3.80:1.00) established that 9.09×10^{-4} mol of isobutylene, 6.95×10^{-5} mol of hydrogen sulfide, 7.3×10^{-4} mol of *tert*-butylthiol, 4.7×10^{-5} mol of di-*tert*-butyl sulfide, 4.0×10^{-5} mol of di-*tert*-butyl disulfide, and 2×10^{-5} mol of isobutane had been generated. The presence of the byproducts detected by NMR was confirmed by GC/MS analysis.

NMR data: *tert*-Butylthiol: ^{1}H NMR δ 1.22 (s, Me_3CSH), 1.62 (s, $Me_3CS\mathit{H}$); $^{13}C\{^1H\}$ NMR δ 34.4 (Me_3CSH), 40.1 ($Me_3\mathit{C}SH$). Isobutylene: ^{1}H NMR δ 1.59 (t, J_{HH} = 1.2 Hz, $\mathit{Me}_2C{=}CH_2$), 4.68 (heptet, J_{HH} = 1.2 Hz, $Me_2C\mathit{CH}_2$); $^{13}C\{^1H\}$ NMR δ 23.5 ($\mathit{Me}_2C{=}CH_2$), 110.5 ($Me_2C{=}\mathit{CH}_2$), 141.2 ($Me_2\mathit{C}{=}CH_2$). Di-*tert*-butyl sulfide: ^{1}H NMR δ 1.32 (s); $^{13}C\{^1H\}$ NMR δ 32.7 ($(\mathit{Me}_3C)_2S$), 45.4 ($(Me_3\mathit{C})_2S$). Di-*tert*-butyl disulfide: ^{1}H NMR δ 1.20 (s); $^{13}C\{^1H\}$ NMR δ 30.1 ($(\mathit{Me}_3C)_2S_2$), 44.6 ($(Me_3\mathit{C})_2S_2$). Isobutane: ^{1}H NMR δ 0.86 (d, J_{HH} = 6.4 Hz, $HC\mathit{Me}_3$); $^{13}C\{^1H\}$ NMR δ 24.4 ($HC\mathit{Me}_3$), 23.1 ($H\mathit{C}Me_3$). Hydrogen sulfide: ^{1}H NMR δ 0.19 (s). These NMR chemical shifts were verified by comparisons with the shifts seen for authentic samples and with published values.[79]

GC/MS data: *tert*-Butylthiol: retention time = 7.1 min; MS peaks at 90, 75, 57, 41, and 29. Isobutylene: retention time = 1.7 min; MS: peaks at 56, 41, and 39. Di-*tert*-butyl sulfide: retention time = 14.3 min; MS peaks at 146, 75, 57, 41, and 29. Di-*tert*-butyl disulfide: retention time = 17.0 min; MS peaks at 178, 122, 57, 41, and 29. Isobutane: retention time = 1.5 min; MS peaks at 43, 42, 41, 28, and 27. Hydrogen sulfide: retention time = 1.0 min; MS peaks at 34, 33, and 32.

***tert*-Butylthiol Dehydrosulfurization Control Experiments.** Films of MoS_2 and TiS_2 were deposited in the static vacuum CVD apparatus as described above, except that the apparatus was maintained under a dynamic vacuum and the NMR tube was not cooled. After the depositions were complete, the apparatus was isolated from the pump, and *tert*-butylthiol (ca. 0.5 g) was introduced while the hot zone was still at 200 °C. After 20 min of interaction between the *tert*-butylthiol and the hot MoS_2 film, the NMR tube was cooled with liquid nitrogen and the volatile products were condensed in; C_6D_6 was added to the NMR tube, which was then flame sealed. ^{1}H and $^{13}C\{^1H\}$ NMR and GC/MS analysis showed that 0.09 equiv of isobutylene and 0.08 equiv of H_2S had been produced per equivalent of *tert*-butylthiol.

The interaction of *tert*-butylthiol and a film of TiS_2 for 20 min at 250 °C yielded approximately 0.04 equiv of isobutylene/equiv of *tert*-butylthiol; only traces of H_2S were detected.

CM970138P

(78) Heller, S. R.; Milne, G. W. A. *EPA/NIH Mass Spectral Data Base*; Washington, D.C.

(79) Pretsch, E.; Clerc, T.; Seibl, J.; Simon, W. *Tables of Spectral Data for Structure Determination of Organic Compounds*, 2nd ed.; Springer-Verlag: New York, 1989.